Astronomy & Astrophysics manuscript no. arXiv
February 7, 2014

Letter to the Editor

The first Frontier Fields cluster: 4.5μm excess in a z ~8 galaxy candidate in Abell 2744

N. Laporte[1,2], A. Streblyanska[1,2], B. Clement[3], I. Pérez-Fournon[1,2], D. Schaerer[4,5], H. Atek[6], F. Boone[4], J.-P. Kneib[6,7], E. Egami[3], P. Martínez-Navajas[1,2], R. Marques-Chaves[1,2], R. Pelló[4], and J. Richard[8]

[1] Instituto de Astrofisica de Canarias (IAC), E-38200 La Laguna, Tenerife, Spain
e-mail: nlaporte@iac.es, alina@iac.es, ipf@iac.es, paloma@iac.es, rmarques@iac.es
[2] Departamento de Astrofisica, Universidad de La Laguna (ULL), E-38205 La Laguna, Tenerife, Spain

[3] Steward Observatory, University of Arizona, 933 N. Cherry Ave, Tucson, AZ 85721, USA
e-mail: bclement@as.arizona.edu, eegami@as.arizona.edu
[4] IRAP, CNRS - 14 Avenue Edouard Belin - F-31400 Toulouse, France
e-mail: roser.pello@irap.omp.eu, frederic.boone@irap.omp.eu
[5] Observatoire de Genéve - 51 Chemin des Maillettes - CH-1290 Sauverny - Switzerland
e-mail: daniel.schaerer@unige.ch
[6] Laboratoire d'Astrophysique, Ecole Polytechnique Fédérale de Lausanne (EPFL), Observatoire de Sauverny, CH-1290 Versoix, Switzerland
e-mail: hakim.atek@epfl.ch,jean-paul.kneib@epfl.ch
[7] Aix Marseille Université, CNRS, LAM (Laboratoire d'Astrophysique de Marseille) UMR 7326, 13388, Marseille, France
[8] CRAL - UMR 5574 - Observatoire de Lyon - 9 avenue Charles André - F-69561 Saint Genis Laval - France
e-mail: johan.richard@univ-lyon1.fr

Received 3 December 2013 / Accepted 31 January 2014

ABSTRACT

Aims. We present in this letter the first analysis of a z ~8 galaxy candidate found in the *Hubble* and *Spitzer* imaging data of Abell 2744, as part of the Hubble Frontier Fields legacy program.
Methods. We applied the most commonly-used methods to select exceptionally high-redshift galaxies by combining non-detection and color-criteria using seven HST bands. We used GALFIT on IRAC images for fitting and subtracting contamination of bright nearby sources.The physical properties have been inferred from SED-fitting using templates with and without nebular emission.
Results. This letter is focussed on the brightest candidate we found (m_{F160W}=26.2) over the 4.9 arcmin^2 field of view covered by the WFC3. It shows a non-detection in the ACS bands and at 3.6μm whereas it is clearly detected at 4.5μm with rather similar depths. This break in the IRAC data could be explained by strong [OIII]+Hβ lines at z ~8 which contribute to the 4.5μm photometry. The best photo-z is found at z ~$8.0^{+0.2}_{-0.5}$, although solutions at low-redshift (z ~1.9) cannot be completely excluded, but they are strongly disfavored by the SED-fitting work. The amplification factor is relatively small at μ=1.49±0.02. The Star Formation Rate in this object is ranging from 8 to 60 $M_\odot.yr^{-1}$, the stellar mass is in the order of $M^\star$=(2.5-10) $\times 10^9$ $M_\odot$ and the size is r ≈0.35±0.15 kpc.
Conclusions. This object is one of the first z ~8 LBG candidates showing a clear break between 3.6μm and 4.5μm which is consistent with the IRAC properties of the first spectroscopically confirmed galaxy at a similar redshift. Due to its brightness, the redshift of this object could potentially be confirmed by near infrared spectroscopy with current 8-10m telescopes. The nature of this candidate will be revealed in the coming months with the arrival of new ACS and Spitzer data, increasing the depth at optical and near-IR wavelengths.

Key words. Galaxies: distances and redshifts - Galaxies: evolution - Galaxies: formation - Galaxies: high-redshift - Galaxies: photometry - Galaxies: star formation

1. Introduction

One of the major topics of modern astronomy is the study of the early Universe through the observation of the first luminous objects. In the last 10 years, several advances have been made to constrain the properties of the Universe during the first billion years and many surveys and instruments have been designed in order to push the boundaries of the observable Universe, e.g. CLASH (Postman et al. 2012), HST Frontier Fields [1], KMOS/ESO (Sharples et al. 2006), or MOSFIRE/Keck (McLean et al. 2012) . These new facilities have helped to strongly increase the number of very high-redshift candidates (z ≥8.0) from a dozen in 2006 (Bouwens & Illingworth 2006) to a hundred in 2013 (eg. Bradley et al. 2012, Oesch et al. 2012). However to date, only 2 objects, among all the z ≥ 7.5 candidates, have been confirmed by spectroscopy (Finkelstein et al. 2013 - F13 hereafter- and Tanvir et al. 2009) but none at z ≥8.5 . Most of the photometric candidates are too faint to be confirmed spectroscopically with current spectrographs, and require the ar-

[1] www.stsci.edu/hst/campaigns/frontier-fields/

rival of future telescopes, such as the JWST[2], the E-ELT [3], or the TMT[4]. Two complementary approaches can be used to select the highest redshift objects: deep blank fields, to select the brightest objects (BoRG survey, Trenti et al. 2011; WUDS survey, Pello et al. in prep), or lensing fields, to take benefit from the cluster magnification on a background source (Kneib & Natarajan 2011, Zheng et al. 2012, Hall et al. 2012).

The Frontier Fields propose to combine the two previous methods by observing 6 lensing clusters and 6 blank fields to a depth similar to the *Hubble Ultra Deep Field* (5σ ~29AB from F435W to F160W). Observations will be spread over 3 years starting in October 2013. The first high-level products have been released on November 1st for the cluster Abell 2744 and a first analysis of these data has been already published by Atek et al. (2013). In this letter we focus on the brightest z ~8 candidate selected in this lensing cluster. In section 2 we present the dataset we used and the data reduction steps we followed to produce high-level quality IRAC data. In section 3, we explain the method we used to select high-redshift galaxy candidates. The z ~8 galaxy candidate and its physical properties are presented and discussed in section 4.

The concordance cosmology is adopted throughout this paper, with Ω_Λ=0.7, Ω_m=0.3 and H_0=70 km s^{-1} Mpc^{-1}. All magnitudes are quoted in the AB system (Oke & Gunn 1983).

2. Data properties

2.1. HST data

This work is based on the December 16th *Space Telescope Science Institute*[5] release which includes 100% of the WFC3 data planned around the lensing cluster Abell 2744. ACS data come from the HST archive as part of program ID : 11689 (PI : R. Dupke) and consist of 6 orbits in F435W and 5 orbits in F606W and F814W respectively. WFC3 data combined two datasets : one from a supernovae search in that field (ID: 13386, PI: S. Rodney) and the Frontier Fields program (ID: 13495, PI: J. Lotz). The depth of each image was computed using noise measurements in thousands empty 0.4" diameter apertures, which not overlapping, on a picture where bright sources were masked (cf. Table 1)

2.2. Spitzer data

Mid-infrared *Spitzer* imaging of Abell 2744 using Infrared Array Camera (IRAC) was obtained on September 2013 as part of the Frontier Field Spitzer program (PI: T. Soifer). The dataset we used in this letter represents 50% of the planned observations for the cluster. We used corrected Basic Calibrated Data (cBCD) images, that are provided by the Spitzer Science Center (SSC) and automatically corrected by pipeline for various artifacts such as muxbleed, muxstripe, and pulldown. The cBCD frames and associated mask and uncertainty images were processed, drizzled (with a factor of 0.65) and combined into final mosaics using the standard SSC reduction software MOPEX. The mosaics have a 3 sigma point source sensitivity (measured from the noise in a clean area) of 0.139 μJy and 0.225 μJy in 3.6μm and 4.5μm respectively.

[2] webpage : www.jwst.nasa.gov/
[3] www.eso.org/public/teles-instr/e-elt/
[4] www.tmt.org
[5] data : http://archive.stsci.edu/prepds/frontier/

Table 1. Properties of *HST* and *Spitzer* data used in this letter.

Filter	$\lambda_{central}$ [μm]	$\Delta\lambda$ [μm]	t_{exp} [ks]	m(5σ)	Instrument
F435W	0.431	0.073	16.16	27.4	ACS
F606W	0.589	0.156	13.25	28.0	ACS
F814W	0.811	0.166	13.25	27.1	ACS
F105W	1.050	0.300	46.52	28.6	WFC3
F125W	1.250	0.300	16.32	28.5	WFC3
F140W	1.400	0.400	22.43	28.7	WFC3
F160W	1.545	0.290	46.57	28.2	WFC3
3.6	3.550	0.750	90.9[a]	0.139[b]	IRAC
4.5	4.493	1.015	90.9[a]	0.225[b]	IRAC

Notes. Informations given in this table : (1) Filter ID, (2) filter central wavelength, (3) filter FWHM, (4) exposure time, (5) depth at 5σ in a 0.4" diameter aperture, (6) instrument
[a] on source
[b] 3σ point source sensitivity in μJy

3. Selection of z ~8 Lyman Break Galaxies

The most successful methods to select high-redshift galaxies is the Lyman Break Technique (Steidel et al. 1999) combining non-detection/detection criteria with color selection. We used SExtractor (Bertin & Arnouts 1996) in double image mode using a weighted sum of F105W and F125W images as detection. The extraction parameters were defined to maximize the number of detections.The catalog contains ~ 6600 detections. The non-detection criteria we applied are :

$$m_{F435W}, m_{F606W}, m_{F814W} > m(2\sigma) \cup m_{F125W} < m(10\sigma) \quad (1)$$

Therefore, in this letter, we limited our search to the bright objects where a F814W-F125W break larger than 1.5mag should be observed, in order to limit the selection of mid-z interlopers (Hayes et al. 2012). We computed the color window by using templates from Bruzual & Charlot (2003), Coleman et al. (1980), Kinney et al. 1996, Polletta et al. (2007) and Silva et al. (1998) Thus the color criteria we adopted were the following :

$$m_{F105W} - m_{F125W} > 0.6 \quad (2)$$
$$m_{F125W} - m_{F160W} < 0.6 \quad (3)$$
$$m_{F105W} - m_{F125W} > 4.6 \times (m_{F125W} - m_{F160W}) - 0.8 \quad (4)$$

Colors were measured on psf-matched data (matched to the worst resolution) using Kron-like apertures. In order to get the total magnitude in each WFC3 bands, we applied aperture corrections using F160W MAG_AUTO following the method described in F13. Among the 21 detections fulfilling the Lyman Break Technique criteria, only two objects are retained after visual inspection.This last step is crucial to remove spurious (eg. all detections in the halo of bright galaxies) and very faint low-redshift objects for which the large optical error bars can explain that they entered our selection criteria. This letter is focussed on the brightest candidate (RA_{J2000} : 00:14:25.083 – DEC_{J2000}: -30:22:49.70). As in F13, we noted that this candidate seems to have a clumpy morphology, with a faint source 0.25" away from the main one (see Figure 1).

Due to the presence of a bright source in the vicinity of our object on the IRAC data (~ 4.4" from the z ~8 candidate), we decided to conduct few additional steps for verifying the Spitzer photometry. We used the galaxy-fitting program GALFIT (Peng et al. 2002) with our own constructed IRAC PSFs for fitting and subtracting all nearby sources around our object in a manner

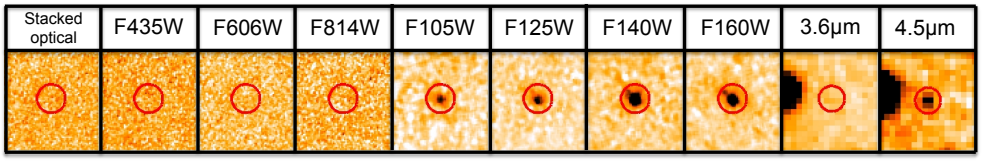

Fig. 1. Postage stamps of the Y_{105}-dropout discussed in this letter. The size of each HST stamp is 2"x2" (7"x7" for the IRAC channels) and the position of the target is displayed by a red circle of 0.4" (ACS and WFC3) and 1.4" (IRAC) radius. We show also the mean stacked optical image computed using the 3 ACS bands.

Table 2. Photometry of the z ~8 galaxy candidate

Filter	F105W	F125W	F140W	F160W	3.6μm	4.5μm
Abell2744_Y1	27.50 ±0.08	26.32 ±0.04	26.26 ±0.03	26.25 ±0.04	>25.48[a]	25.16 ±0.16

Notes. Informations given in this table : Kron-like aperture corrected photometry . Error bars are computed using noise measured in empty apertures around the object.
[a] 3σ limit at the position of our candidate

similar to other high-redshift IRAC studies (e.g., F13). Then, we measured the photometry on residual (contamination-free) image in a 1.4" radius aperture. At 3.6μm, the source is not detected neither in original nor in residual images. If we consider the 4.5μm detection and the 3.6μm 3 sigma limit, the flux ratio is larger than ≈1.3.

4. Physical properties

4.1. Photometric redshift

Photometric redshifts were computed with a new version (v12.2) of the public code *Hyperz* (*New−Hyperz*[6]), originally developped by Bolzonella et al. (2000). The method consists on fitting the SED by a library of 14 templates: 8 evolutionary synthetic SEDs extracted from Bruzual & Charlot (2003), with Chabrier IMF (Chabrier 2003) and solar metallicity ; a set of 4 empirical SEDs compiled by Coleman et al. (1980), and 2 starburst galaxies from the Kinney et al. (1996) library. In case of non-detection in a given band, the flux in this band was set to zero, with an error bar corresponding to the limiting flux.

The best SED-fit is found at z ~7.98 (χ^2_{red}=0.17), with 1σ confidence interval ranging from z ~7.5 to 8.2. We also fitted the SED assuming a low-redshift solution, with z ranging from 0.0 to 3.0. In that configuration the best SED-fit is found at z ~1.92 (χ^2=1.17 - 1σ : 1.7 - 2.1). This z ~8 candidate has a SED remarkably similar to the F13 z ~7.51 galaxy where a strong break is observed in the IRAC data. For these two galaxies, the excess of flux observed at 4.5μm could be explained by contamination due to strong Hβ+[OIII] lines. For the SED fit shown in Fig.2 obtained assuming 1/50 solar metallicity and imposing an age prior of >50 Myr, the [OIII]5007, Hβ restframe equivalent widths are 600 and 190 Å , respectively, which are compatible with the values derived by Smit et al. (2013) from the photometry of seven z ~ 6.6-7 LBGs. At this stage and even if the high-redshift solution seems more likely and the low-z solution disfavored by the SED-fitting work, it appears difficult to conclude definitively on the nature of this source. The arrival of new IRAC data in 2014 will improve the SNR at 3.6μm and help to better understand the nature of this object.

[6] http://userpages.irap.omp.eu/~rpello/newhyperz/

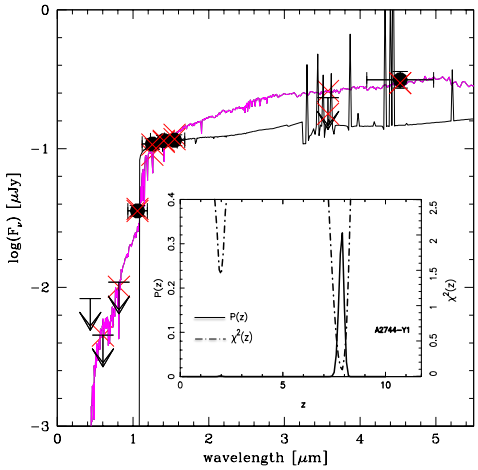

Fig. 2. Fit of the z ~8 galaxy candidate SED at high (black line) and low-redshift (magenta line). ACS upper limits are shown at 1σ and IRAC non-detection is plotted at 3σ. The high-z SED fit shown here is for 1/50 solar metallicity, imposing an age prior of > 50 Myr. The high-redshift solution shows an excess at 4.5μm due to [OIII] and Hβ emission lines as already observed in the z ~7.51 galaxy published in F13. P(z) and $\chi^2(z)$ are also plotted.

4.2. Magnification

One of the interest of using lensing by galaxy clusters to search for very high-redshift galaxies is the magnification by the cluster lens. However this object is relatively far from the cluster core. We estimated an amplification factor of μ=1.49±0.02 using the public lensing model provided by the CATS group (Richard et al., in prep), in the framework of the Frontier Fields. This factor is consistent with those found using other lensing models produced by Merten (μ=1.50), Sharon (μ=1.91), Williams (μ=1.16) and Zitrin (μ=1.33-2.11), confirming a moderate amplification regime for that object.

4.3. Star Formation Rate, Mass and Size

In this section, the SFRs, mass and luminosities are corrected for magnification, and are derived assuming a Salpeter IMF from 0.1–100 $M_\odot$. Overall the quantities derived from SED fits are fairly uncertain, since they depend on assumptions on the metallicity and degeneracies in age–extinction. We therefore only give indicative values for these quantities.

With an absolute UV magnitude M_{1500} = -20.5 the star formation rate is SFR ≈ 8 $M_\odot.yr^{-1}$ using the standard Kennicutt (1998) relation, and without correcting for attenuation by dust. Standard SED fits with solar metallicity models and neglecting nebular emission yield SFR ~ 10 $M_\odot.yr^{-1}$ for a A_V=0.15. When nebular emission is included, following the models of Schaerer & de Barros (2009,2010) the best fits yield SFR ~ 8–60 $M_\odot.yr^{-1}$,

depending on the adopted metallicity and the minimum age imposed. The extinction ranges from $A_V \sim 0.05 - 0.8$, and the expected IR luminosity of this galaxy from $\log(L_{IR}) \sim 9.7$–11.4, as predicted from the amount of energy absorbed in the UV.

The estimated stellar mass is of the order of $M_\star \sim$ (2.5-10) $\times 10^9$ $M_\odot$, when adopting an age prior of t >50 Myr. If younger ages are allowed, which is favored by some best fits, the mass may be a factor 3 lower. Standard SED fits neglecting nebular emission give the largest mass, $M_\star \sim 1 \times 10^{10}$ $M_\odot$. In conclusion, whereas standard models yield a specific SFR, sSFR ~ 1 Gyr^{-1}, the sSFR is ~ 20 times higher with nebular emission (for ages $t > 50$ Myr), and even higher without age constraint. These values are comparable to those derived e.g. by Schaerer & de Barros (2010), de Barros et al. (2012), and Smit et al. (2013) at $z > 6$. The size of this galaxy candidate was computed using SExtractor half-light radius corrected for PSF broadening and GALFIT modeling assuming a Sersic profile. The results are similar (r_{SE} =0.3±0.1 kpc and r_{GAL} =0.35±0.15 kpc after correction for magnification) and in good agreement with other studies of z ~8 galaxies (Ono et al. 2013, Oesch et al. 2010).

5. Discussions

The most common sources of high-redshift sample contamination come from SNe, AGN, low-mass stars, photometric scatter, transient objects, spurious sources, extremely red galaxies, etc. This z ~8 candidate is detected on data taken with two instruments (*HST* and *Spitzer*) limiting the contaminations by spurious sources. Moreover these observations were spread over several weeks allowing us to remove variable and transient sources in our sample. The colors of this source are inconsistent with the colors expected for L,T dwarfs (see figure 1 of Bouwens et al. 2010). Moreover the SExtractor stellarity parameter (CLASS_STAR between 0.1 and 0.2) and the GALFIT work presented above show that our object is resolved at least in the F125W, F140W and F160W bands, which is unlikely for stars.

The expected number of objects in the luminosity regime of this candidate, in the field of view covered by HST and assuming the UV Luminosity Function published by Bouwens et al. 2012 is ~1±1. The comoving volume explored by this survey taking into account the amplification map of the cluster is ~3815 Mpc^3. Therefore the number density of z ~8 galaxies is $\Phi(M_{1500}$=-20.47)=2.6×10^{-4} $mag^{-1}Mpc^{-3}$ (see Atek et al. 2013, for more details) and it is consistent with recent studies published at z ~8 (e.g. Schenker et al. 2013)

The SED of the z ~8 galaxy candidate is comparable to the recent z ~7.5 LBG confirmed by near-IR spectroscopy using MOSFIRE on Keck (F13) regarding the break in magnitude between optical and NIR data (F606W-F105W > 2.5mag) and the detection at 4.5μm combined with the non-detection at 3.6μm with similar depth. Its colors fulfill the color criteria defined by Oesch et al. 2012 and Lorenzoni et al. (2011) and its *intrinsic* SED is similar to the $z \sim 8$ candidates selected in the CANDELS survey (Grogin et al. 2011). Furthermore the H_{160}-[4.5] =1.1 and J_{125} - H_{160} colors are in good agreement with the trend observed by Labbé et al. 2013 for z ~8 objects detected in Spitzer data. As shown in recent papers (e.g. Smit et al. 2013, Clement et al. in prep.) a strong contribution of Hβ and [OIII] emission lines at z >7 to the *Spitzer* photometry could be another argument in favor of the high-redshift solution.

6. Conclusions

Within the 4.9 $arcmin^2$ field of view covered by *HST* in A2744, we found a relatively bright z ~8 galaxy candidate well detected at 4.5μm but undetected at 3.6μm. This excess could be the signature of strong Hβ and [OIII] emission lines in the IRAC channel 2. Based on a SED-fitting work including nebular emission, this object appears as good candidate at z ~8, and its photometric properties, such as Mass, SFR and size, are consistent with expectations at $z > 7$. In the coming months, a new set of ACS and IRAC data will become available and could confirm the break observed. These data will improve the photometry and the overall SED and physical parameters and hopefully will confirm or discard the very high-redshift nature of this source. Most of the $z \sim 8$ sources known to date are too faint to be spectroscopically confirmed with NIR spectrographs, and they require the arrival of new facilities to be confirmed (e.g. JWST or the E-ELT). However this object is bright enough to be explored with current spectrographs in a "reasonable" amount of time (≈10-15h). If the high-redshift solution is confirmed, it will be the second source at z >7.5 with a "break" in IRAC data confirmed.

Acknowledgements. The authors thank the anonymous referee for useful comments, the HST and Spitzer directors and FF teams for their work to make these fantastic data available.This work was supported by the Spanish MINECO under projects AYA2010-21697-C05-04 and FIS2012-39162-C06-02. JPK et HA acknowledges support from the ERC advanced grant LIDA, JR support from the ERC starting grant CALENDS. This work also received support from the French Agence Nationale de la Recherche bearing the reference ANR-09-BLAN-0234.

References

Atek, H., Richard, J., Kneib, J.-P., et al. 2013, ArXiv e-prints
Bertin, E. & Arnouts, S. 1996, A&AS, 117, 393
Bolzonella, M., Miralles, J.-M., & Pelló, R. 2000, A&A, 363, 476
Bouwens, R. J. & Illingworth, G. D. 2006, Nature, 443, 189
Bouwens, R. J., Illingworth, G. D., Oesch, P. A., et al. 2010, ApJ, 709, L133
Bouwens, R. J., Illingworth, G. D., Oesch, P. A., et al. 2012, ApJ, 752, L5
Bradley, L. D., Trenti, M., Oesch, P. A., et al. 2012, ApJ, 760, 108
Bruzual, G. & Charlot, S. 2003, MNRAS, 344, 1000
Chabrier, G. 2003, PASP, 115, 763
Coleman, G. D., Wu, C.-C., & Weedman, D. W. 1980, ApJS, 43, 393
de Barros, S., Schaerer, D., & Stark, D. P. 2012, ArXiv e-prints
Finkelstein, S. L., Papovich, C., Dickinson, M., et al. 2013, Nature, 502, 524
Grogin, N. A., Kocevski, D. D., Faber, S. M., et al. 2011, ApJS, 197, 35
Hall, N., Bradač, M., Gonzalez, A. H., et al. 2012, ApJ, 745, 155
Hayes, M., Laporte, N., Pelló, R., Schaerer, D., & Le Borgne, J.-F. 2012, MNRAS, 425, L19
Kennicutt, Jr., R. C. 1998, ARA&A, 36, 189
Kinney, A. L., Calzetti, D., Bohlin, R. C., et al. 1996, ApJ, 467, 38
Kneib, J.-P. & Natarajan, P. 2011, A&A Rev., 19, 47
Labbé, I., Oesch, P. A., Bouwens, R. J., et al. 2013, ApJ, 777, L19
Lorenzoni, S., Bunker, A. J., Wilkins, S. M., et al. 2011, MNRAS, 414, 1455
McLean, I. S., Steidel, C. C., Epps, H. W., et al. 2012, in Society of Photo-Optical Instrumentation Engineers (SPIE) Conference Series, Vol. 8446, Society of Photo-Optical Instrumentation Engineers (SPIE) Conference Series
Oesch, P. A., Bouwens, R. J., Carollo, C. M., et al. 2010, ApJ, 709, L21
Oesch, P. A., Bouwens, R. J., Illingworth, G. D., et al. 2012, ApJ, 759, 135
Oke, J. B. & Gunn, J. E. 1983, ApJ, 266, 713
Ono, Y., Ouchi, M., Curtis-Lake, E., et al. 2013, ApJ, 777, 155
Peng, C. Y., Ho, L. C., Impey, C. D., & Rix, H.-W. 2002, AJ, 124, 266
Polletta, M., Tajer, M., Maraschi, L., et al. 2007, ApJ, 663, 81
Postman, M., Coe, D., Benítez, N., et al. 2012, ApJS, 199, 25
Schaerer, D. & de Barros, S. 2010, A&A, 515, A73
Schenker, M. A., Robertson, B. E., Ellis, R. S., et al. 2013, ApJ, 768, 196
Sharples, R., Bender, R., Bennett, R., et al. 2006, in Society of Photo-Optical Instrumentation Engineers (SPIE) Conference Series, Vol. 6269, Society of Photo-Optical Instrumentation Engineers (SPIE) Conference Series
Silva, L., Granato, G. L., Bressan, A., & Danese, L. 1998, ApJ, 509, 103
Smit, R., Bouwens, R. J., Labbe, I., et al. 2013, ArXiv e-prints
Steidel, C. C., Adelberger, K. L., Giavalisco, M., Dickinson, M., & Pettini, M. 1999, ApJ, 519, 1
Tanvir, N. R., Fox, D. B., Levan, A. J., et al. 2009, Nature, 461, 1254
Trenti, M., Bradley, L. D., Stiavelli, M., et al. 2011, ApJ, 727, L39
Zheng, W., Postman, M., Zitrin, A., et al. 2012, Nature, 489, 406